Journal of Laser Applications ARTICLE scitation.org/journal/jla

Absorption and temperature distribution during ultrafast laser microcutting of polymeric materials

Cite as: J. Laser Appl. 32, 022044 (2020); doi: 10.2351/7.0000080
Submitted: 1 April 2020 · Accepted: 1 April 2020 ·
Published Online: 4 May 2020

Arifur Rahaman, Xinpeng Du, Boyang Zhou, He Cheng, Aravinda Kar, and Xiaoming Yu

AFFILIATIONS

CREOL, The College of Optics and Photonics, University of Central Florida, Orlando, Florida 32816

Note: This paper is part of the Special Collection: Proceedings of the International Congress of Applications of Lasers & Electro-Optics (ICALEO® 2019).

ABSTRACT

Material processing by ultrafast lasers is an attractive technology for high-precision fabrication, such as cutting, drilling, and surface modification, of a wide range of material, including dielectrics, semiconductor, metals, and polymer composites. However, it is still challenging to apply ultrafast laser processing in many applications because some key processes, such as absorption and heat accumulation, are not fully understood, especially for polymeric materials, which have a low melting temperature and, therefore, are more vulnerable to thermal damage. In this study, an analytical solution to a transient, two-dimensional thermal model is derived using Duhamel's theorem and Hankel's transform method to understand the effect of laser parameters during ultrafast laser interactions with polypropylene (PP), which is a material widely used in many industrial applications. To correlate with theoretical calculation, laser cutting experiments are carried out on PP sheets. This study found that the total energy absorbed in the material and the laser intensity are two important factors to estimate the laser processing performance. In addition, time-resolved measurements are performed by using fast photodiodes and an oscilloscope to understand the dynamics of ultrafast laser interactions during the laser cutting process. Transmitted and reflected signals are monitored and analyzed to extract information on nonlinearity and the absorption coefficient.

Key words: Ultrafast laser, polymer processing, absorption distribution, temperature distribution

I. INTRODUCTION

There has been an increase of using ultrafast lasers in both fundamental research and industrial applications since they were developed in the early 1980s.[1,2] Ultrafast lasers have unique characteristics that offer precision, flexibility, and robustness for processing of wide range of materials, including metals, glasses, polymers, and ceramics, which are not easily achieved by other laser sources.[3,4] Based on the mechanism of laser energy absorption, ultrafast lasers (with the pulse duration in the range of femtoseconds to a few picoseconds, a time scale that is shorter than the thermal equilibrium time in most materials) interact with materials in a way that is fundamentally different from other laser types. The absorption mechanism differs for different materials. For semiconductors and dielectrics that have a large bandgap, the excited electrons can absorb laser energy and bring the material to the plasma state or even produce the Coulomb explosion.[5] For metals, the absorption mechanism is different and the linear absorption contributes the most to laser energy deposition.

Ultrafast laser interactions with polymeric materials have many features, which makes the ultrafast laser system appealing for many industrial applications. As needed for industrial applications, it is required to run the ultrafast laser at a high repetition rate and hence high average power. However, heat accumulation in the material under such processing conditions can deteriorate the processing quality, especially for polymers that typically have a low melting temperature. Therefore, it is important to understand the process physics to efficiently process polymeric material with an ultrafast laser. To determine the thermal effects of different ultrafast laser conditions on a material, an analytical solution of thermal model enables us to represent a direct relation between various laser parameters and the heating process. The analytical solution can be implemented in various industrial applications to monitor and control a given process. The model can be used as a tool that will significantly reduce the time and cost of new process development and avoid

the trial and error approach involving numerous experiments for optimizing process parameters.

Time-resolved measurements of surface reflectivity and transitivity are important for laser applications in material processing, such as welding, cutting, and drilling.[6,7] It has long been recognized that the reflectivity of certain materials can decrease rapidly during irradiation by a high intensity laser beam.[8]

In this paper, an analytical solution to a transient, two-dimensional (2D) thermal model is used for estimating absorption and temperature distribution during ultrafast laser microcutting of polymeric material. In this study, the analytical model is used to analyze the effect of processing parameters, i.e., pulse energy, scanning speed, repetition rate, focal spot size, and pulse duration, during femtosecond laser interaction with polypropylene (PP) sheets, which are important polymeric materials used in many industrial applications, such as plastic parts for various industries including the automotive industry, packaging for consumer products, furniture market, special devices like hinges, and fabrics.[9] To verify the theoretical calculation, laser cutting experiments are carried on PP sheets. Absorption and temperature distribution during ultrafast laser microcutting of polymeric material will be shown for various laser-PP interaction conditions. In addition, time-resolved measurements are performed by using fast photodiodes and an oscilloscope to understand the dynamics of ultrafast laser interactions during the laser cutting process. This study shows the possibility of using ultrafast laser pulses to cut thin polymeric materials with high precision using theoretical and experimental methods.

II. 2D TRANSIENT THERMAL MODELING

In this section, a 2D transient heat conduction model (HCM) and its analytical solution, which describes the effect of the process parameters during ultrashort laser pulse interaction with a workpiece, will be discussed. The details of model development can be found in our previous publication.[10] It is assumed that absorbed laser energy converts to heat instantaneously, and material removal is modeled as a sublimation process where solid material converts directly into vapor.[11] The chemical degradation can occur during the laser processing of polymeric materials.[12] The chemical degradation is treated in the same way as sublimation, because both processes absorb energy and produce gases.[13]

Considering different thermal conductivities in the radial direction, r, and the axial direction, z, the governing heat conduction equation is[14]

$$\frac{\partial^2 T(r,z,t)}{\partial r^2}+\frac{1}{r}\frac{\partial T(r,z,t)}{\partial r}+k_{zr}\frac{\partial^2 T(r,z,t)}{\partial z^2}=\frac{1}{\alpha_r}\frac{\partial T(r,z,t)}{\partial t}, \quad (1)$$

where $k_{zr}=k_z/k_r$ is the ratio of thermal conductivity along z and r; $\alpha_r=k_r/\rho c_p$ is the thermal diffusivity along r; and ρ and c_p are the density and specific heat of the workpiece, respectively.

The boundary conditions (BCs) and the initial condition (IC) are

$$\text{BC1:}\ -k_z\frac{\partial T(r,z,t)}{\partial z}\bigg|_{z=0}=AI(r,t),$$

$$\text{BC2:}\ -k_z\frac{\partial T(r,z,t)}{\partial z}\bigg|_{z=L}=h(T_L-T_\infty),$$

$$\text{BC3:}\ \frac{\partial T(r,z,t)}{\partial r}\bigg|_{r=0}=0,$$

$$\text{IC:}\ T(r,z,0)=T_o,$$

where h is the heat transfer coefficient of the air-workpiece boundary at the lower ($z=L$) surface. Here, T_∞ and T_o are the ambient temperature and initial temperature of the workpiece, respectively, $T_L=T(r,L,t)$, and R_c is the characteristic radius of the cylinder, which is determined in Ref. 10.

The dimensionless parameters are used to reduce the dependency of the solution on a potentially large number of dimensional parameters and are defined as

$$r^*=\frac{r}{\omega_o}\qquad z^*=\frac{z}{\omega_o},$$

$$t^*=\frac{\alpha_r t}{\omega_o^2}\qquad T^*(r^*,z^*,t^*)=\frac{T(r,z,t)-T_\infty}{T_o-T_\infty},$$

where t^* is known as the Fourier number.

The method of solving this HCM is adopted from Ref. 10 to obtain the following dimensionless temperature distribution in the workpiece:

$$T^*(r^*,z^*,t^*)=\sum_{m=1}^{\infty}\frac{J_o(\lambda_m^* r^*)}{N_H(\lambda_m^*)}\bar{\psi}_{ss}^*(\lambda_m^*,z^*,\tau^*)+\sum_{m=1}^{\infty}\frac{J_o(\lambda_m^* r^*)}{N_H(\lambda_m^*)}\sum_{n=1}^{\infty}\frac{\cos(\gamma_n^* z^*)}{N_F(\gamma_n^*)}\tilde{\bar{T}}_i(\lambda_m^*,\gamma_n^*)e^{-at^*}$$
$$-\sum_{m=1}^{\infty}\frac{J_o(\lambda_m^* r^*)}{N_H(\lambda_m^*)}\sum_{n=1}^{\infty}\frac{\cos(\gamma_n^* z^*)}{N_F(\gamma_n^*)}\tilde{\bar{G}}(\lambda_m^*,\gamma_n^*)\int_0^{t^*}e^{-a(t^*-\tau^*)}\frac{d\varphi^*(\tau^*)}{d\tau^*}d\tau^*. \quad (2)$$

All other variables in Eq. (2) are defined in Ref. 10. Equation (2) yields the dimensional temperature distribution in terms of r, z, and t as

$$T(r, z, t) = (T_o - T_\infty)T^*(r^*, z^*, t^*) + T_\infty. \quad (3)$$

III. EXPERIMENTAL SETUP

An Yb:KGW (Yb doped potassium gadolinium tungstate) laser with the wavelength 1030 nm was used to cut commercially available white PP sheets of thickness 300 μm with various laser parameters. Both a knife and a laser beam were used to prepare the cross sections of the laser cut channels. Similar cross sections of the laser cut PP sheets were obtained by both methods; therefore, the sharp knife was used for simplicity.

An experimental setup for ultrafast laser cutting of thin PP sheets is shown in Fig. 1. In this system, an Yb:KGW laser delivers laser pulses of duration tunable from 170 fs to 10 ps with maximum pulse energy of 1 mJ and the repetition rate tunable up to 1 MHz. The maximum average output power is 6 W, and the central wavelength is 1030 nm. In this laser system, the diameter of output laser is 4 mm, which is expanded to 10 mm by a beam expander. An attenuator, which is a variable neural density filter, is used to control the laser power. A lens with 250 mm focal length is used to focus the laser beam, and the PP sheet is placed at the focal plane where the spot size (beam diameter) is measured to be 36.8 μm at $1/e^2$—point and the surface of the PP sheet is kept perpendicular to the laser beam.

The experimental setup for time-resolved measurements is shown in Fig. 2. In this system, the femtosecond laser beam is focused onto the sample with a lens of focal length 250 mm. A beam splitter (10R/90T) and a fast photodiode 1 are used to measure the power of the incident beam, where 10% of incident beam is detected by the photodiode and monitored by a 1-GHz oscilloscope. To study the reflection of the laser beam from the sample, a hemiellipsoidal metallic reflector is used.[15] In this system, the reflector collects both specular and diffusive reflections. The PP sample is placed on the top of a fixture, which is placed at the internal (first) focal point of the elliptical mirror. The sample is tilted at 17° to reduce light backscattering through the entrance hole of the elliptical reflector.

Photodiode 2 detects the reflected laser light, which is located in the external (second) focal point of reflector. To measure the transmission of ultrafast laser through the PP sample, photodiode 3 is placed at the back of the sample.

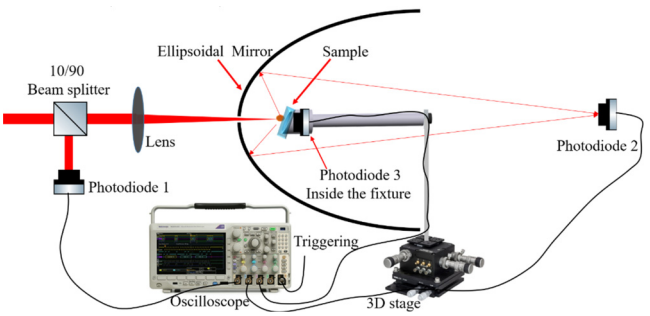

FIG. 2. Experimental setup to measure absorption.

IV. OUTPUTS FROM THE MODEL

The analytical solution [Eq. (3)] is used to model the temperature distributions in the PP sheets due to ultrafast (femtosecond) laser irradiation. The thermophysical properties of PP and laser parameters used in the model are listed in Table I.

The polymeric material undergoes various phase changes during the laser material processing, including chemical decomposition of the atomic bonds in the polymeric chains, thermal degradation, vapor, and a plasma plume consisting of both positive and negative ions and neutral elements. Therefore, the absorption of laser energy will change during the cutting process of the polymeric material. However, thermal properties, such as thermal conductivity, density, and specific heat capacity, are temperature dependent. To simplify the thermal analysis of the ultrashort pulse cutting process, these thermal properties are considered constant in this study.

Results from the thermal model for various laser parameters can be used to examine the maximum depth of cut in the workpiece and the amount of material vaporized using different laser parameters. Figure 3(a) shows the temperature distribution due to ultrafast laser irradiation along the radial direction, r, at the surface ($z = 0$) of the PP sheet for different pulse energies. As input energy to the PP sheet increases with increasing pulse energy, the models

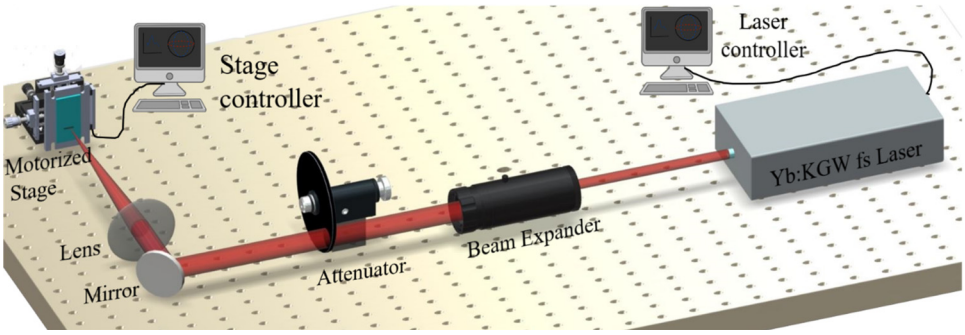

FIG. 1. Schematics of the experimental set for laser cutting of PP sheets.

TABLE I. Laser irradiation parameters and thermophysical properties of PP (Refs. 16 and 17) for thermal modeling.

Properties and parameters	Value
Density of the material, ρ (kg m^{-3})	946
Heat transfer coefficient, h (W/m^2 K)	100
Laser beam radius, ω_o (μm)	18.4
Laser Wavelength, λ (nm)	1030
Pulse duration, t_{on} (fs)	200
Pulse repetition rate, N_p (MHz)	1
Pulse repetition rate, N_p (kHz)	10, 100
Thickness of the PP workpiece (μm)	300
Thermal decomposition temp., T_c (K)	601
Thermal conductivity, k, k_r, k_z (W m^{-1} K^{-1})	0.23
Thermal diffusivity, α (m^2 s^{-1})	1.37×10^{-7}
Specific heat capacity, C_p (J kg^{-1} K^{-1})	1920

produce higher temperature [2.5 μJ in Fig. 3(a)] and maximum intensity is reached at the center of the beam, where the intensity is the highest. Figure 3(b) shows the temperature distribution along the axial direction, z, at the center of the laser beam ($r = 0$), where the highest temperature is reached for each of the pulse energy.

Figure 4 shows the temperature distribution in the workpiece for irradiating laser pulse energy of 2 μJ and a repetition rate of 1 MHz. For this 2D temperature estimation, an interaction time $t_i = 3.68$ ms is used. Here, $t_i = \frac{2\omega_o}{v}$, where v is the laser cutting speed. The region inside the yellow isotherm is higher than the minimum temperature (601 K) required for the PP material to remove, where the thermal decomposition for PP is 600–700 K. Therefore, the partial-depth cutting (D), the kerf width, and the volume of the removal material

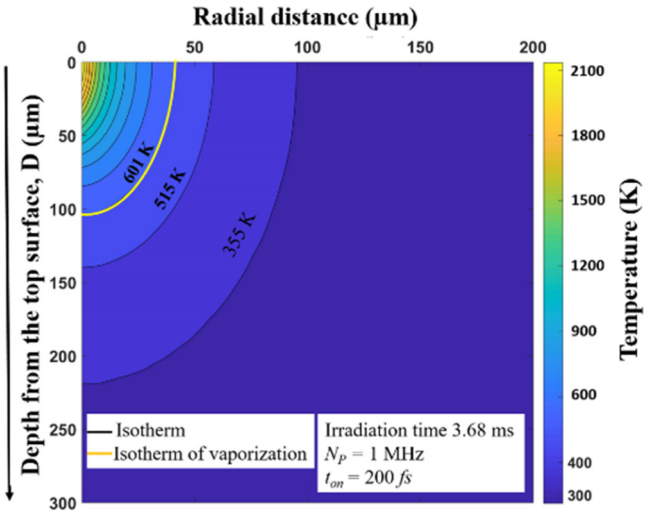

FIG. 4. The temperature distribution in the 2D contour plot in the workpiece for pulse energy 3 μJ, where yellow indicates material removal above the isotherm.

for a given pulse energy can be obtained from a similar contour graph by comparing the known decomposition temperature of PP.

The temperature distribution at the surface of the workpiece ($z = 0$) and the center of the laser beam ($r = 0$) for different pulse energies are shown in Fig. 5(a). Heat accumulation in the workpiece is observed for higher pulse energies. To avoid excessive heating and thermal damage to the material, it is required to optimize the laser parameter to reduce heat accumulation for efficient material

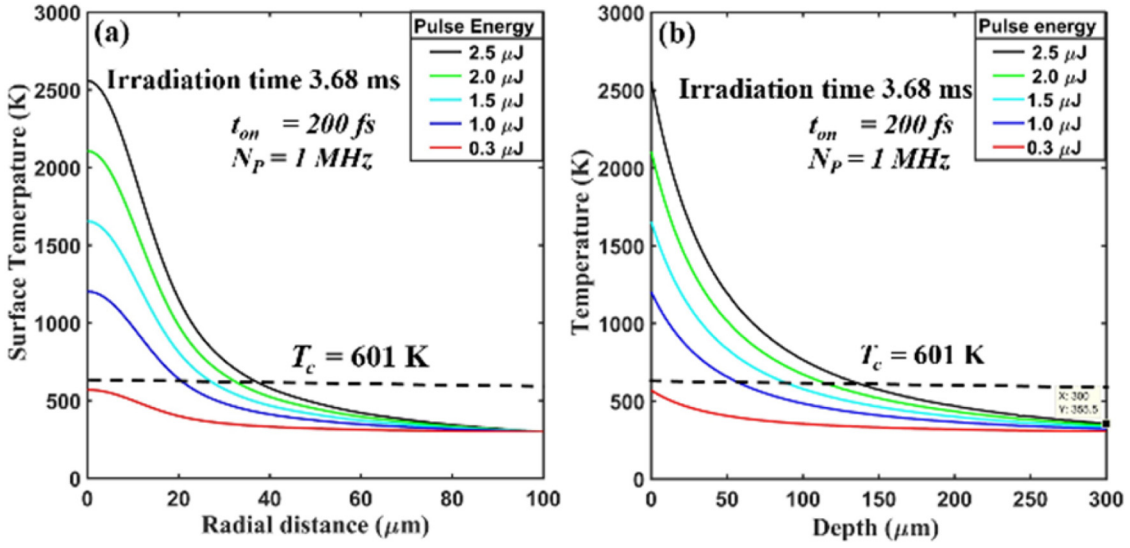

FIG. 3. (a) Radially symmetric temperature distribution at the surface of the workpiece, $z = 0$, and (b) axial temperature distribution at the center of the laser beam, $r = 0$, for different pulse energies from 0.3 to 3 μJ.

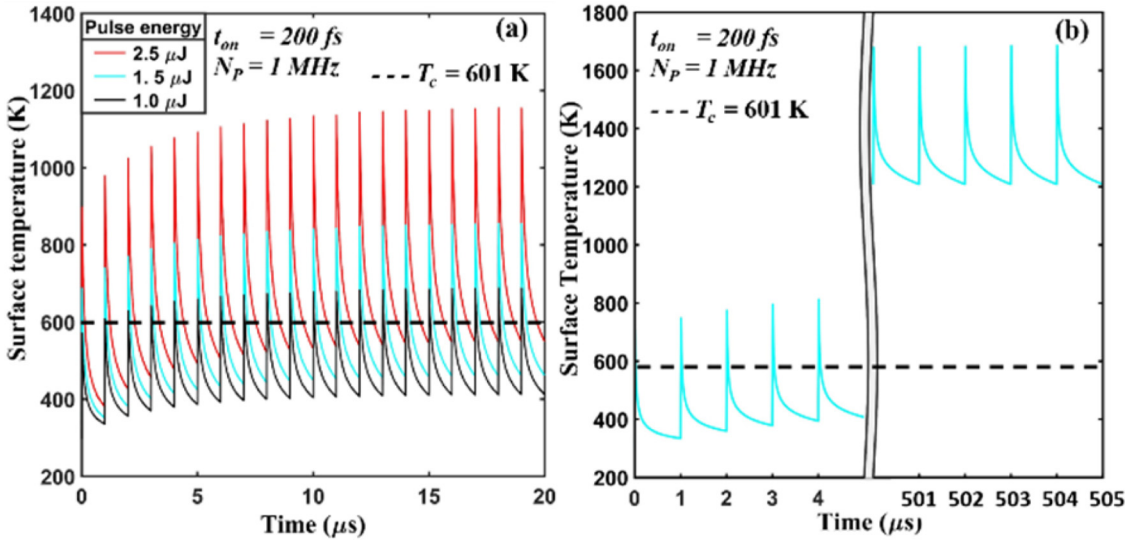

FIG. 5. Temperature distribution over time for different pulse energies at the surface of the workpiece ($z = 0$, $r = 0$) and the decomposition temperature of the PP sheet indicated by a horizontal dash line: (a) heat accumulation with different pulse energies and (b) heat accumulation with 2.5 μJ.

processing. Heat accumulation on the material mostly depends on the pulse energy and pulse repetition.[18–20] Figure 5(b) shows the temperature distribution over time for the pulse energy of 2.5 μJ at the repetition rate of 1 MHz. This figure indicates that the temperature is above the PP decomposition temperature.

V. EXPERIMENTAL RESULTS

To determine the amount of energy absorbed by the PP sheet, the reflected and transmitted signal detected by photodiodes 2 and 3, respectively, are analyzed. The repetition rate of the laser was changed to the single-shot mode. A fresh spot on the sample was irradiated by changing the sample position using a 3D stage. Measurement was started from below-threshold fluence. The damage threshold fluence for this sample is found to be 0.1 J/cm^2 by examining the sample surface with an optical microscope.

Figure 6 shows the absorbance of the PP sample as a function of fluence. To calculate the absorbance (A), measured experimental value of reflectance (R) and transmittance (T) are used, and the relationship $R + T + A = 1$ is used. The absorbance at below-threshold fluence is measured to be 0.3.

The effect of repetition rates of ultrafast laser pulses on laser cutting of PP sheets at 10 mm/s scanning speed is shown in Fig. 7. Figure 7(a) shows the effect of a 10 kHz repetition rate where each of the pulses has larger pulse energy that increases the PP sheet to a high temperature resulting in a large heat affected zone (HAZ). The overlapping area between two successive laser pulses is defined as

$$O_l = 2\omega_o^2\left[\cos^{-1}\left(\frac{v}{2\omega_o N_p}\right) - \left(\frac{v}{2\omega_o N_p}\right)\sqrt{1-\left(\frac{v}{2\omega_o N_p}\right)^2}\right]. \quad (4)$$

Figure 7(b) shows the effect of laser cutting of a PP sheet at 100 kHz, where the overlapping area (99.65%) is higher than that at 10 kHz (96.54%). Better cutting quality is obtained in the case of 100 kHz because the pulse energy for 100 kHz is much lower than that for 10 kHz, even though the pulse overlapping for 100 kHz is higher compared to that for the 10 kHz repetition rate.

In this study, the best cutting results were obtained at 100 kHz with almost no HAZ. The pulse overlapping is too high (99.96%) for the 1 MHz repetition rate that does not allow heat to dissipate

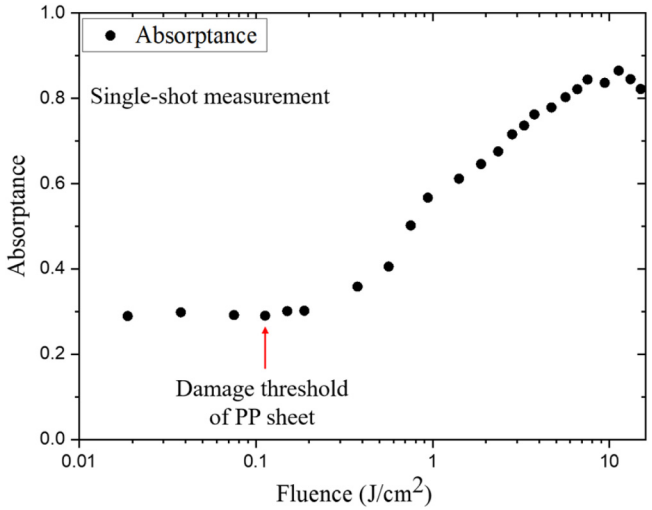

FIG. 6. Absorbance of the PP sample for single femtosecond laser pulses.

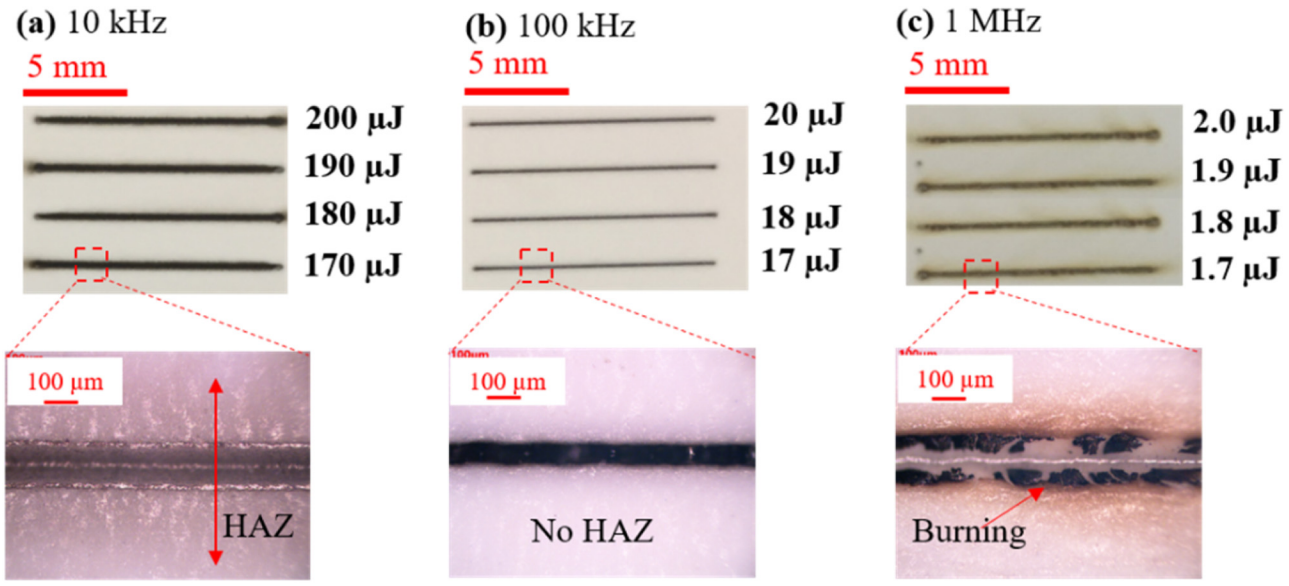

FIG. 7. Experimental observation for the effect of pulse repetition rates on the laser cutting process: (a) HAZ is observed, (b) almost no HAZ and burning, and (c) burning is observed.

in the bulk of the workpiece before the next pulse is incident on the PP sheet resulting in the heat accumulation at the laser material interaction zone, causing thermal damage and burning of the material as shown in Fig. 7(c).

In the case of the 1 MHz repetition rate, the time period between two pulses is very short (1 μs). On the other hand, the 100 kHz repetition rate has a longer time period between two pules. Therefore, the material has sufficient time for heat to

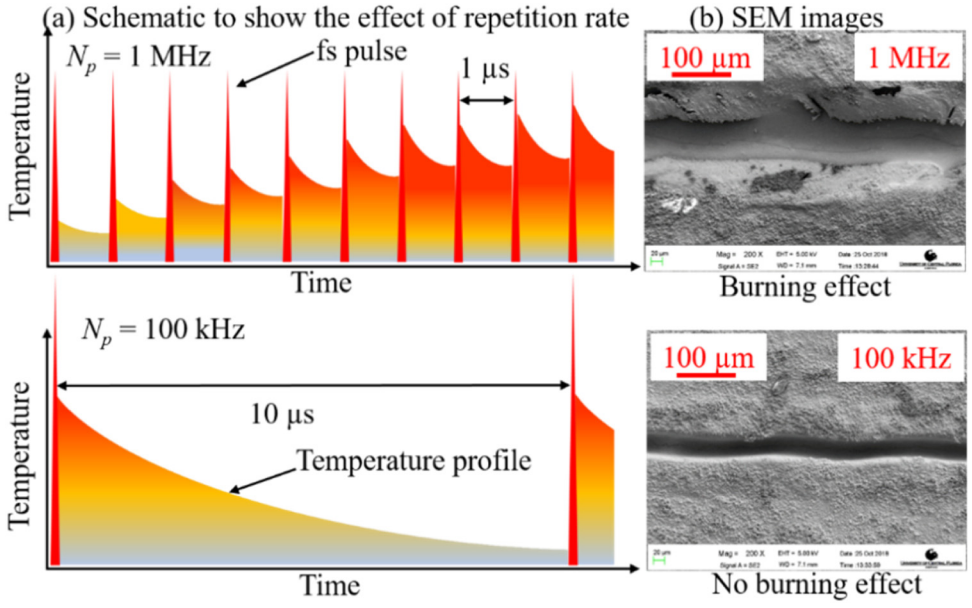

FIG. 8. (a) Schematics of the effect of repetition rate, which indicate the heat accumulation for the higher repetition rate (1 MHz), and (b) SEM images of laser cutting of the PP sheet.

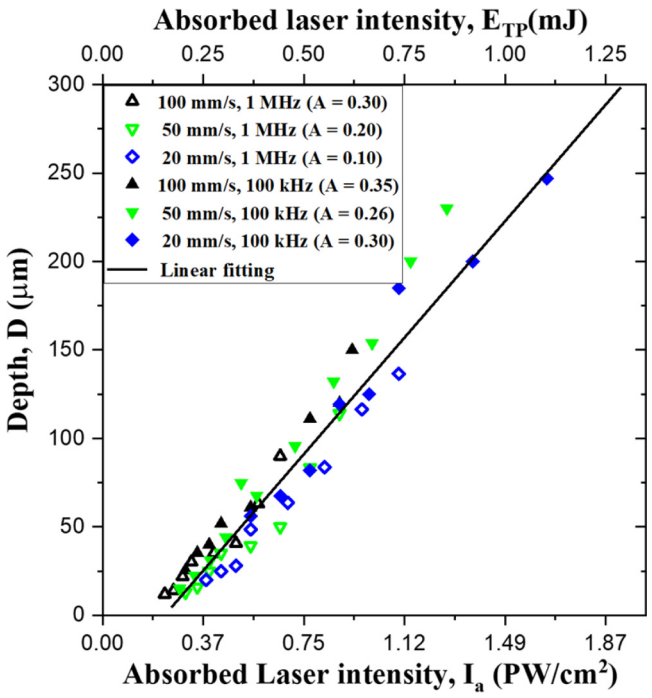

FIG. 9. The depth of the cavity, *D*, formed during the laser cutting at different laser conditions, i.e., cutting speeds and repetition rates, showing that experimental data points for depths follow the same trend as the function of absorbed total energy and the intensity.

dissipate resulting in almost no heat accumulation. Figure 8(a) shows the effect of repetition rate on the laser material interaction. To examine the cut surfaces at a higher magnification, scanning electron microscope (SEM) images are taken and shown in Fig. 8(b). A cleaner kerf is observed for 100 kHz repetition rates, but a wider kerf with a damaged sidewall is obtained in case of the 1 MHz repetition rate. The burning on the surface of the PP sheet is observed in case of the 1 MHz repetition rate, which might induce uncontrolled heating and vaporization of the PP sheets, therefore resulting in thermal damages and a highly tapered profile of the kerf.

In this study, the absorptivities used from the experimental results are for a single shot. However, the absorptivity is expected to vary for multiple pulses and also is temperature dependent. Since vapor and possibly plasma plume are generated at high pulse repetition rates and low cutting speeds, the optical properties of the PP sample, absorptivity, are expected to vary with the different laser processing conditions. The laser beam can be reflected and absorbed with the vapor and plasma plume when the beam passes through these media.[21] Therefore, the amount of the laser energy reaching the surface of the materials is reduced by vapor and plume. In our study, this effect is modeled by lowering the absorptivity of the laser beam on the material so that the amount of the deposited energy as heat in the workpiece is lesser than the incident laser energy.

In this study, the effects of various processing parameters, i.e., pulse repetition rate, scanning speed, pulse energy, and laser beam diameter, were examined by performing different experiments. The depth of the cut of the PP material with ultrafast laser as a function of the "absorbed total pulse energy" (lower *x*-scale), $E_{TP} = \frac{2\omega_o A E_p N_p}{\nu}$, and the "absorbed laser intensity" (upper *x*-scale), $I_a = \frac{2AE_pN_p^{\nu}}{\omega_o \nu t_{op}}$, are shown in Fig. 9. This figure indicates that the experimental data points for the depth measurements of the cavity formed by the removed material coincide into a single straight line for different values of absorptivity under various laser processing conditions of the PP sample. Therefore, this result suggests that the optical effects, i.e., the optical response of the material to the laser parameters, absorptivities, are different, but the thermal effects with the different parameters are similar.

The experimental data points of the depth with different processing conditions are fitted as the following linear equation:

$$D = b(I_a - I_{a_o}), \tag{5}$$

where the slope, *b*, and the threshold absorbed intensity for material removal, I_{a_o}, are found to be 0.0263 cm^3/PW and 0.16 PW/cm^2, respectively. Therefore, this linear relationship will help estimate the "total energy or total intensity" to cut PP sheets of any thickness.

VI. CONCLUSIONS

In this study, the absorption and temperature distribution during ultrafast laser microcutting of polymeric materials (PP sample) are estimated by using an analytical solution to the governing equation for heat transfer due to ultrashort laser pulse heating of solid polymeric material (PP sheets). Both radial and axial temperature distribution at the ultrafast laser irradiate locations are modeled, and the effects of laser processing parameters, such as laser cutting speed and repetition rates, are investigated. It is observed from the experimental studies that a repetition rate of 100 kHz gives the best quality cut compared to the other repetition rates in the study, where the 100 kHz repetition rate is capable of producing clean and thorough cut of the PP sample at the pulse energies of tens of microjoules. The depths of the cut collapse into a single straight line as a function of the total absorbed intensity and energy for various process parameters. Therefore, this study will help to estimate the process parameters of PP sheets during ultrafast laser processing.

REFERENCES

[1]K. Sugioka and Y. Cheng, "Ultrafast lasers—Reliable tools for advanced materials processing," Light Sci. Appl. **3**, 1–12 (2014).
[2]W. Sibbett, A. A. Lagatsky, and C. T. A. Brown, "The development and application of femtosecond laser systems," Opt. Express **20**, 6989–7001 (2012).
[3]S. Mishra and V. Yadava, "Laser beam micro-machining (LBMM)—A review," Opt. Lasers Eng. **73**, 89–122 (2015).
[4]R. R. Gattass and E. Mazur, "Femtosecond laser micromaching in transparent materials," Nat. Photonics **2**, 219–225 (2008).
[5]N. M. Bulgakova, R. Stoian, A. Rosenfeld, I. V. Hertel, and E. E. B. Campbell, "Electronic transport and consequences for material removal in ultrafast pulsed laser ablation of materials," Phys. Rev. B **69**, 054102 (2004).
[6]J. F. Ready, "Change of reflectivity of metallic surface during Irradiation by CO_2-TEA laser pulses," J. Qantum Electron. **12**, 137–142 (1976).

[7]G. E. Jellison, D. H. Lowndes, D. N. Mashburn, and R. F. Wood, "Time resolved reflectivity measurements on silicon and germanium using a pulsed excimer KrF laser heating beam," Phys. Rev. B **34**, 2407–2415 (1986).
[8]O. Benavides, O. Lebedeva, and V. Golikov, "Reflection of nanosecond Nd:YAG laser pulses in ablation of metals," Opt. Express **19**, 21842–21848 (2011).
[9]H. A. Maddah, "Polypropylene as a promising plastic: A review," Am. J. Polym. Sci. **6**, 1–11 (2016).
[10]A. Rahaman, A. Kar, and X. Yu, "Thermal effects of ultrafast laser interaction with polypropylene," Opt. Express **4**, 5764–5784 (2019).
[11]V. I. Mazhukin, I. Smurov, C. Surry, and G. Flamant, "Overheated metastable states in polymer sublimation by laser radiation," Appl. Surf. Sci. **86**, 7–12 (1995).
[12]Y. K. Godovsky, *Thermophysical Properties of Polymers* (Springer, New York, 1992).
[13]C. Zhang, I. A. Salman, N. R. Quick, and A. Kar, "Two-dimensional transient modeling of CO2 laser drilling of microvias in high density flip chip substrates," in *ICALEO (LIA), Miami, FL, 31 October–3 November 2005* (Laser Institute of America, Orlando, FL, 2005), pp. 404–411.
[14]M. N. Özişik and D. W. Hahn, *Heat Conduction* (Wiley, New York, 2010).
[15]L. B. Guo, C. M. Li, W. Hu, Y. S. Zhou, B. Y. Zhang, Z. X. Cai, X. Y. Zeng, and Y. F. Lu, "Plasma confinement by hemispherical cavity in laser-induced breakdown spectroscopy," Appl. Phys. Lett. **98**, 131501 (2011).
[16]S. Zhang and A. R. Horrocks, "A review of flame retardant polypropylene fibers," Prog. Polym. Sci. **28**, 1517–1538 (2003).
[17]C. Maier and T. Calafut, *Polypropylene: The Definitive User's Guide and Data* (Elsevier, New York, 2008).
[18]S. M. Eaton, H. Zhang, and P. R. Herman, "Heat accumulation effects in femtosecond laser-written waveguides with variable repetition rate," Opt. Express **13**, 4708–4716 (2005).
[19]F. Bauer, A. Michalowski, T. Kiedrowski, and S. Nolte, "Heat accumulation in ultra-short pulsed scanning laser ablation of metals," Opt. Express **23**, 1035–1043 (2005).
[20]L. L. Taylor, R. E. Scott, and J. Qiao, "Integrating two-temperature and classical heat accumulation models to predict femtosecond laser processing of silicon," Opt. Mater. Express **8**, 648–658 (2018).
[21]A. Kar, J. A. Rothenflue, and W. P. Latham, "Scaling laws for thick-section cutting with a chemical oxygen-iodine laser," J. Laser Appl. **9**, 279–286 (1997).